ELSEVIER

Marine Micropaleontology 41 (2001) 9–23

MARINE MICROPALEONTOLOGY

www.elsevier.nl/locate/marmicro

The last occurrence of *Proboscia curvirostris* in the North Atlantic marine isotope stages 9-8

N. Koç[a,*], L. Labeyrie[b], S. Manthé[b], B.P. Flower[c], D.A. Hodell[d], A. Aksu[e]

[a]*Norwegian Polar Institute, Polar Environmental Centre, N-9296 Tromsø, Norway*
[b]*Centres des Faibles Radioactivites, CNRS-CEA, Gif sur Yvette, France*
[c]*Department of Marine Science, University of South Florida, 140 Seventh Avenue South, St. Petersburg, FL 33701, USA*
[d]*Department of Geology, University of Florida, 1112 Turlington Hall, Gainesville, FL 32611, USA*
[e]*Department of Earth Sciences, Centre for Earth Resources Research, Memorial University of Newfoundland, St. John's, Newfoundland, Canada A1B 3X5*

Received 19 April 2000; accepted 16 October 2000

Abstract

Well-preserved diatoms are present in high sedimentation rate Pleistocene cores retrieved on Ocean Drilling Program (ODP) Legs 151, 152, 162 and IMAGES cruises of R/V *Marion Dufresne* from the North Atlantic. Investigation of the stratigraphic occurrence of diatom species shows that the youngest diatom event observed in the area is the last occurrence (LO) of *Proboscia curvirostris* (Jousé) Jordan and Priddle. *P. curvirostris* is a robust species that can easily be identified in the sediments, and therefore can be a practical biostratigraphic tool. We have mapped its areal distribution, and found that it stretches from 40°N to 80°N in the North Atlantic. Further, we have correlated the LO *P. curvirostris* to the oxygen isotope records of six cores to refine the age of this biostratigraphic event. The extinction of *P. curvirostris* is latitudinally diachronous through Marine Isotope Stages (MIS) 9 to 8 within the North Atlantic. This is closely related to the paleoceanography of the area. *P. curvirostris* first disappeared within interglacial MIS 9 (324 ka) from the northern areas that are most sensitive to climatic forcing, like the East Greenland current and the sea–ice margin. It survived in mid-North Atlantic until the conditions of the MIS 8 (glaciation) became too severe (260 ka). In the North Pacific at ODP Site 883 the LO *P. curvirostris* falls within MIS 8. The observed overlap in age between the North Atlantic and the North Pacific strongly suggests that the extinction of *P. curvirostris* is synchronous between these oceans.

Keywords: biostratigraphy; North Atlantic; diatoms; Pleistocene; paleoceanography; isotope stratigraphy; oxygen

1. Introduction

During the last decade several high-sedimentation rate sites were drilled on sediment drifts of the North Atlantic and the Nordic Seas to study the evolution of millennial-scale climate variability (i.e. Myhre et al., 1995; Jansen et al., 1996). Most of these sites have well preserved calcium carbonate and siliceous microfossils, which provide excellent opportunities for refining the resolution of the North Atlantic

* Corresponding author.
E-mail addresses: nalan.koc@npolar.no (N. Koç), laurent.labeyrie@cfr.cnrs-gif.fr (L. Labeyrie), bflower@marine.usf.edu (B.P. Flower), hodell@nersp.nerdc.ufl.edu (D.A. Hodell), aaksu@sparky2.esd.mun.ca (A. Aksu).

0377-8398/01/$ - see front matter
PII: S0377-8398(00)00054-2

biostratigraphic schemes. Based on Ocean Drilling Program (ODP) Sites 919 and 983 eight Pleistocene diatom datum events were identified and, for the first time, tied directly to the oxygen isotope stratigraphy of the sites (Koç and Flower, 1998; Koç et al., 1999). On the basis of these datums, four high-latitude North Atlantic diatom zones were proposed for the Pleistocene (Koç and Flower, 1998; Koç et al., 1999).

The latest diatom datum event recognised in the Pleistocene sediments of mid-high latitudes of both the North Pacific and the North Atlantic is the last occurrence (LO) of *Proboscia curvirostris* (Jousé) Jordan and Priddle (1991) (Koizumi, 1992; Koç et al., 1999). In this study we investigate further the suitability of this species as a biostratigraphic marker and the event as a biostratigraphic datum. We do this by mapping the areal distribution of *P. curvirostris* in North Atlantic sediments, and by correlating the LO *P. curvirostris* event in six high-resolution North Atlantic sediment cores to their oxygen isotope stratigraphies to refine the timing of the event (Fig. 1).

2. Previous records of *Proboscia curvirostris* in the North Atlantic

A good biostratigraphic marker should be easily identifiable and dissolution-resistant. Further, it should have a wide areal distribution and a short life span. *Proboscia curvirostris* (Jordan and Priddle, 1991: p. 57; synonym: *Rhizosolenia curvirostris* Jousé 1959, p. 48, pl. 2, fig. 17; Akiba and Yanagisawa, 1986, p. 497, pl. 42, figs. 1, 2; pl. 45, figs. 1–6), like all other fossil *Proboscia* species, is a robust and dissolution-resistant species. Due to its tubular structure, termed a "proboscis", and marked curvature and the spines, it is also easily identifiable in the sediments (Fig. 2).

Proboscia curvirostris is recorded from DSDP/ODP Sites 552, 606, 607, 609, 610, 611 (Baldauf, 1984; 1987), 646 (Monjanel and Baldauf, 1989), 919 (Koç and Flower, 1998), 981, 982 (Koç, unpublished data), 983 (Koç et al., 1999), and from MD952014 and MD952027 (this study) in the North Atlantic (Fig. 1). In the Nordic Seas it is recorded from ODP Sites 907 (Koç and Scherer, 1996) and 986 (Jansen et al., 1996), and from MD992278 and MD992285 (Koç, unpublished data). This suggests quite a wide distribution for *P. curvirostris* in the North Atlantic stretching from 40°N to 80°N (Fig. 1).

3. Material

Six high-resolution cores with well preserved diatoms and detailed oxygen isotope stratigraphies were chosen for documentation of the LO *Proboscia curvirostris* in the North Atlantic (Fig. 1, Table 1). Even though *P. curvirostris* is recorded from several other sites in the North Atlantic, these sites are not used to document the LO *P. curvirostris* since the resolution of the biostratigraphic studies are too coarse for the present study. These sites are only used to document the distribution of *P. curvirostris* in the North Atlantic.

Sites MD952027 and DSDP 609 are located beneath the present North Atlantic Drift flow (Fig. 1). Core MD952027 consists of nanno bearing detri-carbonate silty clay, and has sedimentation rates of 18 m/100 ka. (Bassinot and Labeyrie, 1996). The upper 164 m of DSDP 609 consists of interbedded oozes, marls, and muds with sedimentation rates of 6 m/100 ka (Baldauf et al., 1987). Sites MD952014 and ODP 983 are located on the Bjorn Drift under the influence of the Irminger Current. These drift sites have sedimentation rates of 15 m/100 ka. The sediments at the Bjorn Drift and at Site 983 are predominantly composed of rapidly accumulated fine-grained terrigeneous particles and minor amounts of biogenic material (Jansen et al., 1996; Wold, 1994). Since the sediment build-up mainly consists of erosion and deposition of terrigeneous material from the Icelandic slope, resedimentation of biogenic material should be minimal. Further, there is no sedimentological evidence for erosion or winnowing at these sites (Jansen et al., 1996). ODP Site 919 is located on the continental rise of Southeast Greenland, within the western part of the Irminger Basin. It is primarily under the influence of the East Greenland Current. Sediments at this site are composed predominantly of silty clay, clayey silt, and clay with silt (Larsen et al., 1994). Sedimentation rates at this site are in the order of 18 m/100 ka. ODP Site 646 is situated on the northern flank of the Eirik Ridge, which is one of

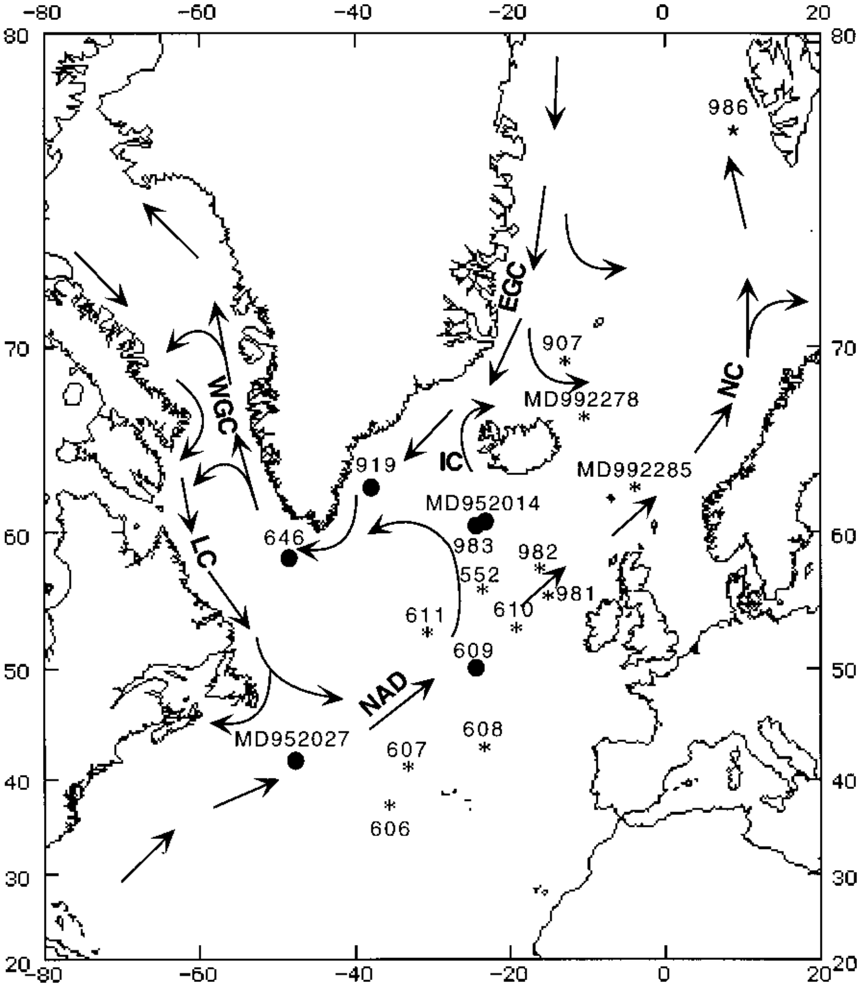

Fig. 1. Map of the northern North Atlantic Ocean. Plotted are the general surface circulation and the location of the cores where *Proboscia curvirostris* is observed. In cores marked with dots the last occurrence of *P. curvirostris* is correlated to the oxygen isotope stratigraphy of the core. MD depicts cores taken by the French RV Marion Dufresne during the IMAGES cruises. All other cores are Deep Sea Drilling (DSDP) or Ocean Drilling Program (ODP) cores. Surface currents are illustrated with arrows as follows: NAD = North Atlantic Drift; IC = Irminger Current; NC = Norwegian Current; EGC = East Greenland Current; WGC = West Greenland Current; LC = Labrador Current.

the large sediment drifts in the northwest Atlantic. The site is influenced by the present-day subarctic West Greenland Current. Sediments at this site and at Eirik Ridge are dominantly terrigeneous clay and silt (Srivastava and Arthur et al., 1987; Wold, 1994). Sedimentation rates are in the order of 10 m/100 ka. Since most of the studied drift sites are build-up of erosion and deposition of terrigeneous material, we do not think resedimentation of biogenic material is a problem at these sites.

4. Methods

ODP Sites 919, 983 and MD952014 and MD952027 were sampled at intervals of 0.3–1.5 m to locate the LO *Proboscia curvirostris*. The sampled intervals from individual cores and the abundance of diatoms are listed in Appendix A. In DSDP Site 609 and ODP Site 646 previously published LO levels of *P. curvirostris* were used (Baldauf, 1987; Monjanel and Baldauf, 1989). The sample intervals where the

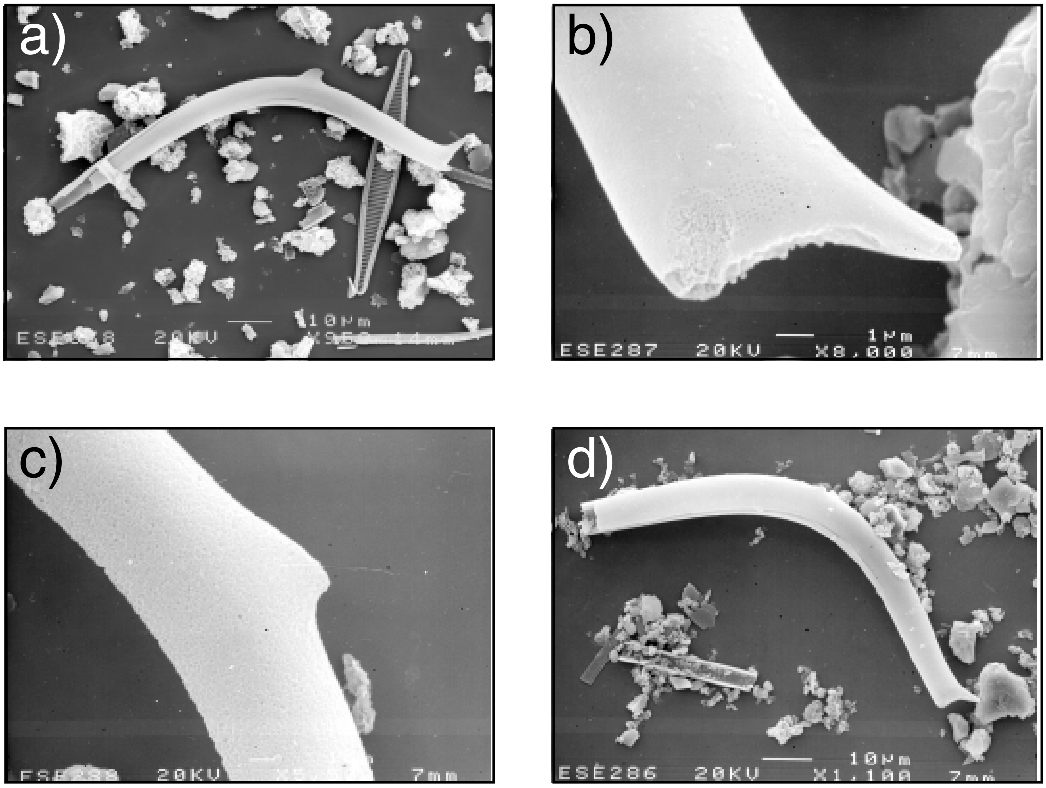

Fig. 2. Scanning electron microscope (SEM) photographs of *Proboscia curvirostris* Jordan and Priddle: (a) *P. curvirostris* Jordan and Priddle and *Nitzschia fossilis* (Frenguelli) Kanaya on the right side, Sample 162-983A-9H-3, 49–50 cm; (b) Detail showing a dentate end in Sample 152-919A-7H-7, 40–41 cm; (c) Detail showing a triangular spine, Sample 152-919A-7H-7, 40–41 cm; (d) *P. curvirostris* Jordan and Priddle, Sample 152-919A-7H-7, 40–41 cm.

LO *P. curvirostris* is observed in individual cores are listed in Table 2. Results from ODP Site 983 was previously published (Koç et al., 1999). In addition to the previously published results from ODP Site 919 (Koç and Flower, 1998), this site was resampled in higher resolution between 36 and 46 mbsf around the LO level of *P. curvirostris*. Approximately 1–2 g of dry sample was acid cleaned and mounted on a $4 \times 2.4\ \text{cm}^2$ glass for diatom investigations. The whole slide area was scanned, and qualitative abundance estimates of individual taxa were recorded. Details of the methods for diatom cleaning and counting procedures for these cores are previously published (Koç and Flower, 1998; Koç et al., 1999). Smear slides with $4 \times 2.4\ \text{cm}^2$ dimensions were used for samples from cores MD952014 and MD952027. Qualitative abundance estimates of diatoms followed the same procedures as the other cores.

Table 1
Positions of those cores where the last occurrence of *Proboscia curvirostris* is correlated to the oxygen isotope stratigraphy of the core

Core site	Latitude	Longitude	Water depth (m)
DSDP 609	49°53′N	24°14′W	3883
ODP 646A	58°12N	48°22 W	3458
ODP 919A	62°40.20′N	37°27.61′W	2088
ODP 983A	60°24.20′N	23°38.43′W	1985
MD 95-2014	60°34.93′N	22°04.52′W	2397
MD 95-2027	41°44.67′N	47°24.79′W	4112

Stable oxygen isotope records of the cores are measured at the Laboratoire des Sciences du Climat et de l’Environnement, CNRS by L. Labeyrie and S. Manthé (DSDP 609, MD95-2014, MD95-2027), University of South Florida by B.P. Flower (ODP

Table 2
The last occurrence of *Proboscia curvirostris* recorded in the North Atlantic sediments

Site	Top		Bottom		Age (ka)
	Core, section, interval (cm)	Depth (mbsf)	Core, section, interval (cm)	Depth (mbsf)	
ODP 919A	5H-6, 38–39	44.38	5H-6, 68–70	44.68	313–317
MD 95-2014		30.94		31.60	308–314
ODP 983A	4H-2, 49–50	28.39	4H-3, 49–50	29.89	276–299
MD 95-2027		32.70		33.00	258–260
DSDP 609[a]	2H-3, 43–45	12.02	2H-4, 43–45	13.52	240–263
ODP 646A[b]	1H-CC	5.0	3H-1, 128–130	17.0	28–258

[a] DSDP 609 from Baldauf, 1987.
[b] ODP 646A from Monjanel and Baldauf, 1989.

919), University of Florida by D.A. Hodell (ODP 983) and at the Memorial University of Newfoundland by A. Aksu (ODP 646). All records are measured on planktonic foraminifer species. Stable oxygen isotope records of ODP 919, ODP 646, MD95-2014 are measured on *Neogloboquadrina pachyderma* (sinistral) (Koç and Flower, 1998; Aksu et al., 1989; unpublished LSCE data, respectively), that of core DSDP 609 is measured on *N. pachyderma* (dextral) (Koç et al., 1999), that of core MD95-2027 is measured on *Globigerina bulloides* (unpublished LSCE data), that of core ODP 983 is measured on *N. pachyderma* and *G. bulloides* (Channell et al., 1997).

5. Results

The LO of *Proboscia curvirostris* occurs within Marine Isotope Stages (MIS) 9 and 8 in the investigated cores (Fig. 3). At ODP Site 919, which is a site at present influenced by the cold East Greenland current, and at site MD952014 south of Iceland this event happens within the second half of MIS 9, and is dated to 317–308 ka (after Imbrie et al., 1984; Prell et al., 1986; Martinson et al., 1987) (Table 2). This is the earliest timing recorded for this event in the investigated cores. At ODP Site 983 the extinction of *P. curvirostris* takes place around the MIS 9/8 transition dated between 299 and 276 ka. Further south, at ODP/DSDP Sites 646, 609 and MD952027 the LO of *P. curvirostris* does not occur until towards the end of MIS 8 between 263 and 240 ka. At MD952027, where we have the highest sampling resolution, the event takes place between substages 8.4 and 8.2, and is dated to 260–258 ka. A similar timing is observed also at DSDP Site 609 and ODP Site 646, where the LO *P. curvirostris* is recorded between substages 8.4 and 8.2. However, due to the larger sampling interval in these cores the event can not be dated as tightly as in MD952027.

From these results it is clear that the extinction of *Proboscia curvirostris* is latitudinally diachronous within the North Atlantic, and is closely related to the paleoceanography of the area. *P. curvirostris* first disappeared from northern areas that are most sensitive to climatic forcing, like the East Greenland current and the sea–ice margin. But survived in mid-North Atlantic until the conditions of the MIS 8 glaciation became too severe. This pattern of climate evolution is similar to that of MIS 5, where the surface ocean waters of the Nordic Seas cool much earlier than the mid-latitude North Atlantic (Cortijo et al., 1994). We believe that this type of climate evolution most probably explains the diachronity observed in the extinction of *P. curvirostris* through MIS 9 and 8.

6. Discussion and conclusions

Proboscia curvirostris has also a middle to high latitude distribution in the North Pacific. Its last occurrence can be a valuable datum for correlation between the high-latitude North Atlantic and the North Pacific Oceans. Morley et al. (1982) and Sancetta and Silvestri (1984) dated the extinction

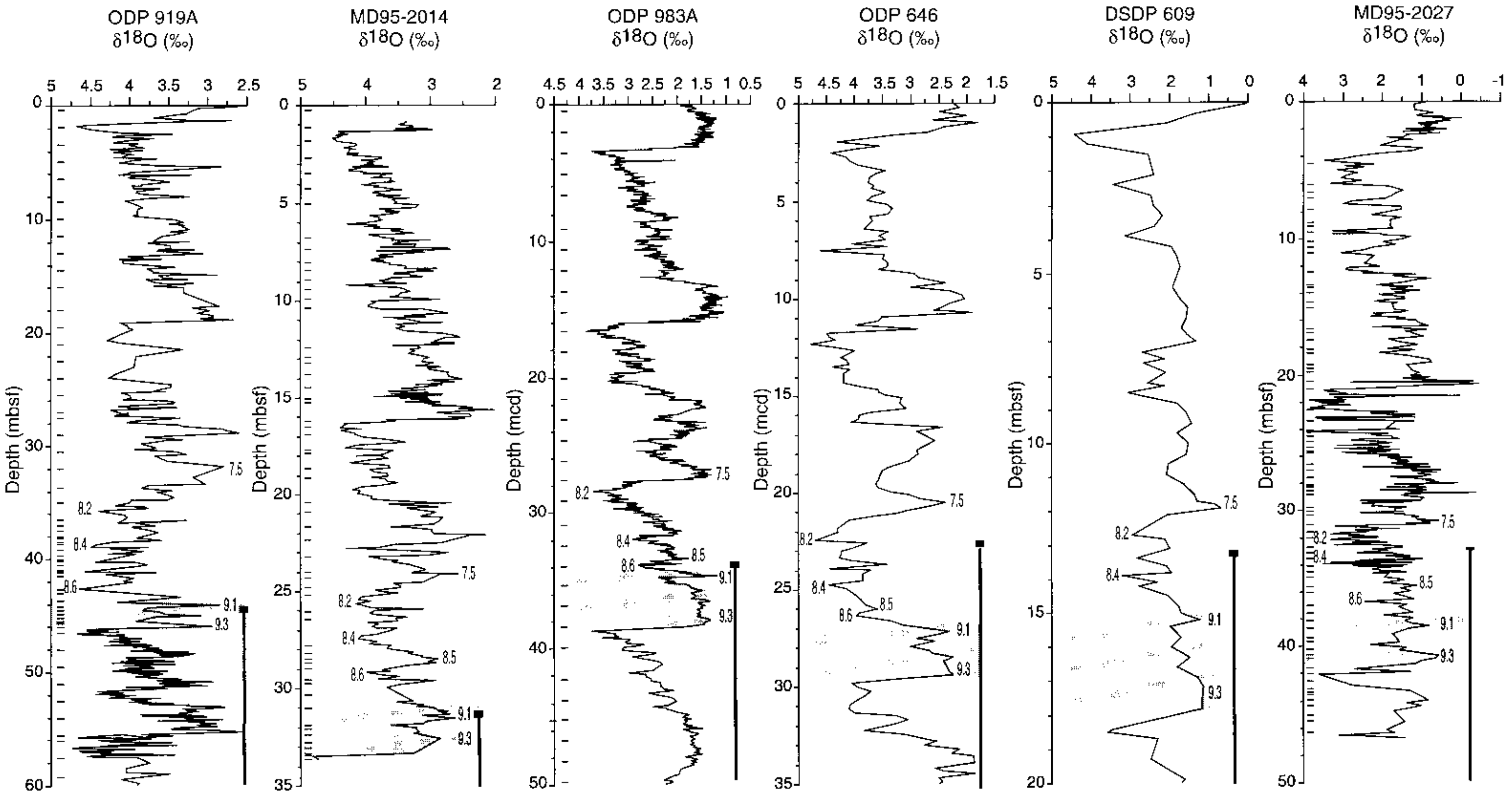

Fig. 3. The last occurrence (LO) of *Proboscia curvirostris* plotted on the oxygen isotope stratigraphy of each core. Oxygen isotope records of cores ODP 919 (Flower, unpublished data), ODP 646 (Aksu et al. 1989), MD95-2014 (unpublished LSCE data) are measured on *Neogloboquadrina pachyderma*(sinistral), that of core DSDP 609 (Koç et al., 1999) is measured on *N. pachyderma* (dextral), that of core MD95-2027 is measured on *Globigerina bulloides* (unpublished LSCE data), that of core ODP 983 is measured on *N. pachyderma* and *G. bulloides* (Channell et al., 1997). Marine isotope stage 9 is shaded, and the substages numbered according to Prell et al. (1986). Sampling intervals are plotted as bars on the left side of the records.

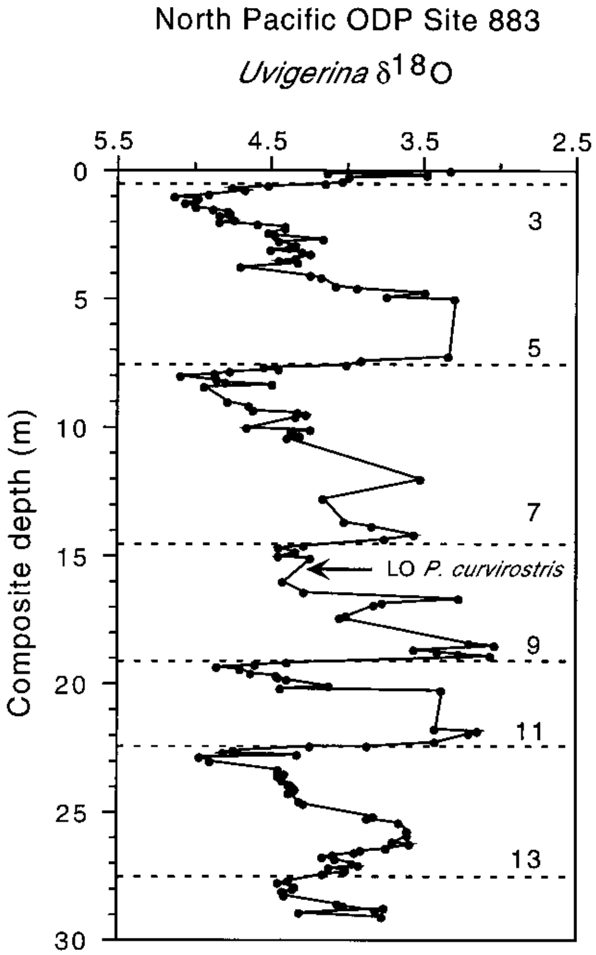

Fig. 4. Oxygen isotope record of ODP Site 883 plotted together with the last occurrence (LO) of *Proboscia curvirostris* (Keigwin, 1995; Morley et al., 1995). Numbers refer to oxygen isotope stages.

of *P. curvirostris* at 0.276 Ma and correlated it to MIS 8 from cores in the subarctic region of the North Pacific. Several other authors have dated the LO of *P. curvirostris* to 0.250–0.300 Ma in the middle-high latitude North Pacific (Akiba, 1986; Koizumi and Tanimura, 1985; Koizumi, 1986; Yanagisawa and Akiba, 1998). However, the event was not correlated directly to the oxygen isotope stratigraphy of the sites investigated. At present the only site in the North Pacific where this event can be correlated to the oxygen isotope stratigraphy of the site is ODP Site 883 from the Detroit Seamount where an upper Quaternary oxygen isotope record is generated by Keigwin (1995). Morley et al. (1995) recorded the LO of *P. curvirostris* in Hole 883B at 15.56 mbsf and dated the event to the early portion of MIS 8 through the correlation of % *Cycladophora davisiana* pattern and the oxygen isotope records of Holes 883C and D. We translated this level to the composite depth scale of the oxygen isotope record of Site 883 through the correlation of the magnetic susceptibility records of the four Site 883 holes shown in Fig. 1 of Keigwin (1995). We also find that at ODP Site 883 the LO of *P. curvirostris* takes place within early MIS 8 (Fig. 4).

Bearing the dating uncertainties of these sites in mind, we propose that the observed overlap in age between the North Atlantic and the North Pacific strongly suggests that the LO of *Proboscia curvirostris* falls within MIS 9-8 in both oceans. These results indicate that there is a high possibility that this event is synchronous (within the uncertainties of paleoceanographic influences which caused diachronity in its extinction within MIS 9-8) between these two oceans, and therefore the datum can be used for inter-ocean correlation.

Even though the observed diachronity of LO of *Proboscia curvirostris* in the North Atlantic can be explained by paleoceanography, why it became extinct in both the North Atlantic and the North Pacific Oceans exactly within MIS 9-8 can not be explained so readily. *P. curvirostris* was not the only species which went extinct during this period. *Thalassiosira jouseae* Akiba also went extinct around the same time with *P. curvirostris* both in the North Atlantic and in the North Pacific, signalling that a large scale environmental change had taken place in MIS 9-8 (Koizumi, 1992; Koç et al., 1999). As indicated by ice volume reconstructions, MIS 8 was not an especially severe glaciation. In fact the previous glaciations MIS 10 and MIS 12 were more severe (McManus et al., 1999). Still, *P. curvirostris* survived MIS 10 and 12, but not MIS 8. It is possible that even though the ice volume reconstructions indicate more severe glaciations during MIS 10 and 12, the surface ocean conditions were not accordingly severe. Alternatively, some other environmental factor played a stronger role in this species extinction in MIS 8.

Acknowledgements

We are grateful to Julianne Fenner and José-Abel Flores for their constructive comments, which helped prepare the final version of the manuscript. We thank Audun Igesund for the preparation of Fig. 2. The study material was provided by the Ocean Drilling Program and the IMAGES Program. This work was supported by grants from the Norwegian Research Foundation, Norwegian Polar Institute and the Norwegian Petroleum Directory to N. Koç, and by the University of South Florida Research and Creative Scholarship Grant Program under Grant No. 1245 940 R3 (BPF) to B. Flower.

Appendix A

Notes: B = barren, T = trace, R = rare, F = few, C = common, A = abundant

Core, section, interval (cm)	Depth (mbsf)	*Proboscia curvirostris* abundance	Diatom abundances
ODP Hole 919A			
1H-1, 41–42	0.410	B	C
1H-2, 40–41	1.900	B	B
1H-3, 41–42	3.410	B	T
1H-4, 40–41	4.900	B	B
1H-5, 41–42	6.410	B	A
2H-1, 41–42	8.410	B	C
2H-2, 40–41	9.900	B	A
2H-3, 41–42	11.410	B	C
2H-4, 40–41	12.900	B	F
2H-5, 41–42	14.410	B	A
2H-6, 41–42	15.910	B	A
3H-1, 39–40	17.890	B	C
3H-2, 38–39	19.380	B	B
3H-3, 39–40	20.890	B	B
3H-4, 39–40	22.390	B	B
3H-5, 40–41	23.900	B	F
3H-6, 40–41	25.400	B	C
3H-7, 42–43	26.920	B	C
4H-1, 39–40	27.390	B	C
4H-2, 40–41	28.900	B	F
4H-3, 40–41	30.400	B	C
4H-4, 41–42	31.910	B	C
4H-5, 43–44	33.430	B	C
4H-6, 41–42	34.910	B	F
4H-7, 40–41	36.400	B	C
5H-1, 39–40	36.890	B	C
5H-1, 88–90	37.390	B	F
5H-1, 128–130	37.790	B	C
5H-2, 8–10	38.090	B	B
5H-2, 38–39	38.380	B	F
5H-2, 48–50	38.490	B	C
5H-2, 108–110	39.090	B	A
5H-3, 8–10	39.590	B	C
5H-3, 39–40	39.890	B	R
5H-3, 46–48	39.970	B	F
5H-3, 88–90	40.390	B	B
5H-3, 126–128	40.770	B	C
5H-4, 8–10	41.090	B	C
5H-4, 40–41	41.400	B	A
5H-5, 8–10	42.590	B	C
5H-5, 40–41	42.900	B	A
5H-5, 108–110	43.580	B	C
5H-6, 8–10	44.080	B	C
5H-6, 38–39	44.380	B	F
5H-6, 68–70	44.680	F	C

(*continued*)

Core, section, interval (cm)	Depth (mbsf)	*Proboscia curvirostris* abundance	Diatom abundances
5H-6, 108–110	45.090	R	C
5H-6, 128–130	45.290	F	C
5H-6, 148–150	45.490	F	A
5H-7, 8–10	45.580	F	C
5H-7, 28–30	45.780	F	C
5H-7, 35–36	45.850	F	A
6H-1, 39–40	46.390	B	B
6H-2, 40–41	47.900	B	B
6H-3, 40–41	49.400	B	R
6H-4, 40–41	50.900	B	R
6H-5, 40–41	52.400	F	C
6H-6, 40–41	53.900	F	C
6H-7, 40–41	55.400	B	B
7H-1, 41–42	55.910	B	R
7H-2, 40–41	57.400	B	B
7H-3, 48–49	58.980	B	B
7H-4, 40–41	60.400	B	B
7H-5, 40–41	61.900	R	F
ODP Hole 983A			
1H-1, 49–50	0.490	B	A
1H-2, 49–50	1.990	B	C
1H-3, 49–50	3.490	B	B
1H-4, 49–50	4.990	B	F
1H-5, 49–50	6.490	B	F
2H-1, 49–50	9.080	B	A
2H-2, 49–50	10.580	B	A
2H-3, 49–50	12.080	B	C
2H-4, 49–50	13.580	B	A
2H-5, 49–50	15.080	B	A
2H-6, 49–50	16.580	B	B
2H-7, 48–49	18.070	B	B
3H-1, 49–50	20.050	B	R
3H-2, 49–50	21.550	B	A
3H-3, 49–50	23.050	B	A
3H-4, 49–50	24.550	B	F
3H-5, 49–50	26.050	B	C
3H-6, 49–50	27.550	B	B
3H-7, 49–50	29.050	B	R
4H-1, 49–50	30.850	B	R
4H-2, 49–50	32.350	B	C
4H-3, 49–50	33.850	F	C
4H-4, 49–50	35.350	F	A
4H-5, 49–50	36.850	R	A
4H-6, 49–50	38.350	B	B
4H-7, 49–50	39.850	B	B
5H-1, 49–50	42.200	A	A
5H-2, 49–50	43.700	A	A
5H-3, 49–50	45.200	C	A
5H-4, 49–50	46.700	C	A
5H-5, 49–50	48.200	C	A
5H-6, 49–50	49.700	C	A

(*continued*)

Core, section, interval (cm)	Depth (mbsf)	*Proboscia curvirostris* abundance	Diatom abundances
5H-7, 49–50	51.200	B	B
MD95-2014			
	20.0	B	R
	110.0	B	F
	180.0	B	R
	260.0	B	C
	340.0	B	C
	420.0	B	A
	500.0	B	C
	670.0	B	R
	730.0	B	A
	800.0	B	B
	840.0	B	F
	890.0	B	R
	930.0	B	B
	980.0	B	R
	1030.0	B	F
	1232.0	B	B
	1280.0	B	B
	1315.0	B	F
	1370.0	B	R
	1437.0	B	C
	1495.0	B	C
	1520.0	B	F
	1618.0	B	B
	1640.0	B	B
	1680.0	B	F
	1760.0	B	F
	1780.0	B	R
	1860.0	B	R
	1910.0	B	B
	2030.0	B	C
	2080.0	B	C
	2160.0	B	B
	2230.0	B	R
	2310.0	B	F
	2390.0	B	F
	2424.0	B	F
	2469.0	B	F
	2510.0	B	F
	2592.0	B	R
	2634.0	B	C
	2770.0	B	F
	2810.0	B	R
	2840.0	B	F
	2860.0	B	C
	2884.0	B	C
	2950.0	B	F
	2961.0	B	C
	3024.0	B	F
	3094.0	B	C

(*continued*)

Core, section, interval (cm)	Depth (mbsf)	*Proboscia curvirostris* abundance	Diatom abundances
	3160.0	C	A
	3183.0	B	B
	3200.0	C	A
	3230.0	C	A
	3270.0	C	A
	3300.0	C	A
	3327.0	F	C
	3340.0	B	B
	3356.0	B	B
MD95-2027			
	1.0	B	F
	450.0	B	C
	600.0	B	C
	650.0	B	C
	696.0	B	F
	780.0	B	C
	870.0	B	C
	900.0	B	R
	945.0	B	C
	1010.0	B	F
	1050.0	B	R
	1100.0	B	R
	1230.0	B	F
	1340.0	B	R
	1350.0	B	R
	1390.0	B	F
	1460.0	B	F
	1500.0	B	F
	1650.0	B	B
	1680.0	B	R
	1740.0	B	R
	1800.0	B	B
	1830.0	B	C
	1924.0	B	C
	1950.0	B	C
	1970.0	B	A
	2040.0	B	B
	2100.0	B	F
	2250.0	B	C
	2253.0	B	C
	2330.0	B	R
	2400.0	B	F
	2414.0	B	A
	2450.0	B	F
	2480.0	B	F
	2530.0	B	R
	2550.0	B	F
	2575.0	B	C
	2660.0	B	B
	2700.0	B	B
	2750.0	B	T

(*continued*)

Core, section, interval (cm)	Depth (mbsf)	*Proboscia curvirostris* abundance	Diatom abundances
	2810.0	B	F
	2820.0	B	F
	2850.0	B	R
	2880.0	B	R
	2970.0	B	R
	3000.0	B	C
	3030.0	B	B
	3100.0	B	C
	3150.0	B	F
	3200.0	B	C
	3270.0	B	C
	3300.0	F	C
	3350.0	R	C
	3400.0	R	C
	3450.0	C	A
	3480.0	F	A
	3550.0	R	F
	3600.0	B	R
	3700.0	R	F
	3750.0	R	F
	3800.0	R	F
	3860.0	B	F
	3930.0	B	F
	3960.0	F	F
	4020.0	C	C
	4050.0	C	C
	4090.0	C	C
	4150.0	C	C
	4200.0	C	C
	4250.0	F	F
	4300.0	B	B
	4330.0	B	R
	4350.0	C	C
	4390.0	F	F
	4430.0	B	B
	4500.0	F	F
	4540.0	B	R
	4620.0	R	F

Appendix B

Core ODP 919 Depth (mbsf)	*N. pachyderma* (s.) $\delta^{18}O$(‰)
0.0900	2.6287
0.2800	3.1175
0.4900	3.2053
0.6900	3.2747
0.8900	3.4453

(*continued*)

Core ODP 919 Depth (mbsf)	*N. pachyderma* (s.) $\delta^{18}O$(%.)
1.0800	3.6903
1.2800	3.1753
1.3000	2.6981
1.4800	3.5073
1.5800	4.0103
1.7000	4.4947
1.7800	4.6733
1.9800	4.5313
2.1800	4.4133
2.3800	4.0843
2.4600	3.4545
2.5800	4.1613
2.7800	4.2073
2.8000	3.6945
3.0800	4.0883
3.2000	4.1998
3.2800	3.9003
3.4800	4.0003
3.6800	3.8183
3.7600	4.2485
3.8800	3.9613
3.9600	3.8371
4.0800	4.2053
4.2800	3.9513
4.3000	4.0259
4.4800	4.0953
4.5800	4.1923
4.7000	3.6527
4.7800	3.9333
5.0000	4.1283
5.1800	3.6533
5.3800	2.8293
5.7800	3.9933
5.8000	3.9380
6.0600	4.1313
6.1000	3.2132
6.2000	3.9638
6.2800	4.0123
6.4800	3.7935
6.6800	3.4893
6.8800	3.8357
6.9700	3.8445
7.0800	3.9711
7.2800	3.9410
7.3000	3.6135
7.4800	3.9061
7.5600	3.9137
7.7800	3.8420
7.9500	3.2314
8.0800	3.7339
8.2800	4.0505
8.6800	3.9066

(*continued*)

Core ODP 919 Depth (mbsf)	*N. pachyderma* (s.) $\delta^{18}O$(%.)
8.8800	3.8334
9.0800	3.8881
9.2800	3.9068
9.5800	3.8934
9.6400	3.9624
9.7800	3.798
9.9800	3.4100
10.180	3.3104
10.380	3.4868
10.450	3.3018
10.580	3.3281
10.780	3.2381
11.090	3.4807
11.130	3.2758
11.290	3.4338
11.480	3.5780
11.680	3.6447
11.880	3.6998
11.950	3.2352
12.080	3.7594
12.280	3.4794
12.490	3.4755
12.580	3.6186
12.640	3.1678
12.780	3.6588
12.980	3.0531
13.180	4.0216
13.340	3.8284
13.440	4.1250
13.510	3.5934
13.580	4.0877
13.780	4.0798
14.080	3.6507
14.130	3.4165
14.280	3.7698
14.480	3.7052
14.680	3.6963
14.880	2.8825
14.940	3.6267
15.080	3.5564
15.200	3.2578
15.280	3.7873
15.470	3.6858
15.580	3.5658
15.630	3.1744
15.780	3.6910
15.980	3.3064
16.430	3.2949
17.560	2.8472
17.580	2.9553
17.780	3.1866
17.980	2.9734

(*continued*)

Core ODP 919 Depth (mbsf)	*N. pachyderma* (s.) $\delta^{18}O$(‰)
18.180	3.1216
18.380	2.9920
18.450	2.9230
18.580	2.9261
18.690	3.0835
18.750	2.6644
18.980	3.4281
19.060	3.9714
19.080	4.1130
19.280	4.0493
19.300	4.0248
19.480	4.0144
19.680	3.9468
19.950	4.086
20.580	4.2802
20.800	4.1125
21.460	3.3138
22.080	3.9186
22.960	3.9415
23.580	4.1688
23.950	4.2591
24.470	3.4633
24.740	3.4764
24.980	3.6486
25.060	3.6919
25.070	3.5442
25.280	4.0931
25.480	3.9960
25.680	3.9840
25.880	4.0670
25.950	3.5189
26.050	3.4243
26.220	3.4406
26.480	4.1314
26.560	3.985
26.580	3.3939
26.780	4.2245
27.260	4.0169
27.080	4.0167
27.270	4.1852
27.470	3.3527
27.680	3.9405
27.870	4.0307
28.050	3.3678
28.260	3.3067
28.300	3.0998
28.480	2.8073
28.580	2.7573
28.780	2.5914
29.170	3.7908
29.370	3.3251
29.450	3.4833

(*continued*)

Core ODP 919 Depth (mbsf)	*N. pachyderma* (s.) $\delta^{18}O$(‰)
29.580	3.5855
29.760	3.8423
30.100	3.6653
30.250	3.7378
30.280	3.9211
30.480	3.3930
30.680	3.2757
30.860	3.6754
31.250	3.5157
31.580	3.1287
31.780	2.7926
32.180	2.9462
32.770	3.1801
33.280	3.0291
33.490	3.7570
33.700	3.8448
33.800	3.6554
33.950	3.4510
34.080	3.6474
34.280	3.5196
34.470	3.4248
34.580	3.4400
34.760	3.5199
34.780	3.9742
34.980	4.0001
35.180	4.1752
35.380	3.8001
35.450	3.7636
35.580	4.1425
35.770	4.3820
36.080	4.0615
36.320	4.0286
36.800	4.1414
36.580	3.2749
36.780	3.9144
36.980	3.6781
37.180	3.9689
37.380	3.7757
37.450	3.7036
37.580	3.6411
37.780	3.6997
38.080	3.8947
38.280	3.5898
38.480	4.1952
38.680	4.4183
38.880	4.4852
38.950	3.7582
39.080	4.2320
39.280	3.8162
39.480	4.2587
39.580	3.9259
40.200	4.4263

(*continued*)

Core ODP 919 Depth (mbsf)	*N. pachyderma* (s.) δ^{18}O(%.)
40.230	3.9411
40.430	3.7752
40.580	3.8705
41.080	4.5576
41.180	3.6655
41.280	4.2960
41.700	3.9487
41.880	4.0737
42.080	3.9705
42.580	4.6372
43.380	3.3529
43.780	4.1378
44.080	2.8452
44.280	3.7703
44.480	3.8256
44.680	3.6282
44.880	3.5313
44.950	3.0926
45.080	3.6874
45.480	3.9038
45.950	2.941
46.030	3.7375
46.080	3.8948
46.160	4.5175
46.220	4.5275
46.280	4.2776
46.360	4.5375
46.410	4.4775
46.480	4.1367
46.510	4.6575
46.610	4.5775
46.680	4.0723
46.760	4.2775
46.820	4.0775
46.880	4.0387
46.950	4.1275
46.970	3.8427
47.030	4.1975
47.080	4.1649
47.160	4.0675
47.220	3.8675
47.280	4.2523
47.350	3.9875
47.410	4.0675
47.480	3.9797
47.520	3.7975
47.580	4.3159
47.660	3.7275
47.720	3.9475
47.780	3.8527
47.860	3.6375
47.920	3.8175

(*continued*)

Core ODP 919 Depth (mbsf)	*N. pachyderma* (s.) δ^{18}O(%.)
47.980	3.5937
48.060	3.5775
48.130	3.9775
48.180	3.2464
48.260	3.6875
48.330	3.5875
48.380	3.1697
48.430	3.253
48.460	3.6075
48.470	3.2397
48.530	3.5775
48.580	3.3148
48.660	3.7875
48.730	4.0475
48.780	3.9201
48.850	4.0075
48.920	4.0175
48.980	3.5559
49.020	4.1067
49.080	3.4265
49.160	4.2167
49.220	4.1167
49.280	3.4199
49.360	4.0767
49.420	3.8067
49.480	3.7237
49.560	3.7867
49.630	4.0567
49.680	3.6884
49.760	4.0967
49.830	4.2067
49.880	3.5264
49.960	3.9567
49.970	3.6295
50.020	4.0267
50.080	3.575
50.160	3.8767
50.280	3.6380
50.360	3.9129
50.520	3.7129
50.580	3.3290
50.660	3.6429
50.720	3.6329
50.780	2.9370
50.860	3.5529
50.920	3.6129
50.980	3.1607
51.060	3.5429
51.120	3.5629
51.180	3.0070
51.260	4.0429
51.320	3.9529

(*continued*)

Core ODP 919 Depth (mbsf)	*N. pachyderma* (s.) $\delta^{18}O$(‰)
51.380	3.5260
51.450	3.5829
51.580	4.0090
51.660	4.3529
51.710	4.4029
51.780	4.0838
51.860	4.4229
51.980	3.9220
52.020	4.2429
52.080	3.9850
52.160	4.1029
52.220	4.2529
52.280	3.6095
52.360	3.9729
52.420	3.8129
52.480	3.7728
52.560	4.0029
52.620	3.9129
52.700	3.4470
52.760	3.8329
52.820	3.6929
52.880	3.2440
52.960	3.2329
52.970	2.8271
52.990	2.9899
53.020	3.2629
53.080	2.7880
53.160	3.0729
53.220	3.3129
53.280	3.1490
53.360	3.2729
53.420	3.2029
53.480	3.1203
53.520	3.3533
53.580	3.2540
53.660	3.3767
53.720	3.8667
53.780	3.0583
53.860	3.8367
53.920	3.4367
53.980	3.0230
54.060	3.2867
54.120	3.2067
54.180	2.8130
54.260	3.6367
54.280	3.0364
54.320	3.3367
54.380	3.1427
54.580	2.8920
54.660	3.1367
54.780	2.8850
54.920	3.3867

(*continued*)

Core ODP 919 Depth (mbsf)	*N. pachyderma* (s.) $\delta^{18}O$(‰)
55.020	3.4596
55.080	2.8923
55.280	2.5370
55.360	3.1427
55.480	3.8417
55.570	3.4516
55.710	3.8197
55.520	4.0898
55.580	4.3960
55.660	4.6095
55.720	4.6491
55.780	3.7360
55.860	4.1967
55.920	3.9303
55.980	4.3937
56.120	4.2710
56.180	3.4670
56.260	4.0170
56.380	4.2730
56.450	4.2471
56.460	3.4055
56.520	4.6078
56.580	4.5850
56.660	4.7279
56.720	4.6145
56.780	3.9380
56.860	4.6387
56.920	4.5153
56.980	4.5977
57.010	4.2417
57.100	4.3676
57.170	4.1480
57.220	3.4303
57.280	3.7712
57.310	4.2755
57.380	4.5390
57.450	4.1829
57.480	3.8997
57.950	3.7482
58.480	4.0477
58.780	4.0457
58.980	3.4917
59.380	4.1087
59.780	3.8787
60.480	4.0437
60.970	3.3068
61.480	4.2757
61.980	2.6477
62.450	3.3001
63.980	3.8067
64.940	3.0950

References

Akiba, F., 1986. Middle Miocene to Quaternary diatom biostratigraphy in the Nankai Trough and Japan Trench, and modified Lower Miocene through Quaternary diatom zones for middle-to-high latitudes of the North Pacific. Init. Rep. DSDP 87, 393–481.

Akiba, F., Yanagisawa, Y., 1986. Taxonomy, morphology and phylogeny of the Neogene diatom zonal marker species in the middle-to-high latitudes of the North Pacific. Init. Rep. DSDP 87, 483–554.

Aksu, A.E., de Vernal, A., Mudie, P.J., 1989. High-resolution foraminifer, palynologic, and stable isotopic records of upper Pleistocene sediments from the Labrador Sea: paleoclimatic and paleoceanographic trends. Proc. ODP, Sci. Results 105, 617–652.

Baldauf, J.G., 1984. Cenozoic diatom biostratigraphy and paleoceanography of the Rockall Plateau region, North Atlantic, Deep Sea Drilling Project, Leg 81. Init. Rep. DSDP 81, 439–478.

Baldauf, J.G., 1987. Diatom biostratigraphy of the middle and high-latitude North Atlantic Ocean, Deep Sea Drilling Project, Leg 94. Init. Rep. DSDP 94, 729–762.

Baldauf, J.G., Thomas, E., Clement, B., Takayama, T., Weaver, P.P.E., Backman, J., Jenkins, G., Mudie, P.J., Westberg-Smith, M.J., 1987. Magnetostratigraphic and biostratigraphic synthesis, Deep Sea Drilling Project Leg 94. Init. Rep. DSDP 94, 1159–1205.

Bassinot, F., Labeyrie, L., 1996. IMAGES MD 101, Les rapports de campagnes á la mer. I'Institut Français pour la Recherche et la Technologie Polaires, 96-1, 217 pp.

Channell, J.E.T., Hodell, D.A., Lehman, B., 1997. Relative geomagnetic paleointensity and $\delta^{18}O$ at ODP Site 983 (Gardar Drift, North Atlantic) since 350 ka. Earth Planet. Sci. Lett. 153, 103–118.

Cortijo, E., Duplessy, J.C., Labeyrie, L., Leclaire, H., Duprat, J., van Weering, T.C.E., 1994. Eemian cooling in the Norwegian Sea and North Atlantic ocean preceding continental ice-sheet growth. Nature 372, 446–449.

Imbrie, J., Hays, J.D., Martinson, D.G., McIntyre, A., Mix, A.C., Morley, J.J., Pisias, N.G., Prell, W., Shackleton, N.J., 1984. The orbital theory of Pleistocene climate: support from a revised chronology of the marine $\delta^{18}O$ record. In: Berger, A. (Ed.), Milankovitch and Climate. Reidel, Dordrecht.

Jansen, E., Raymo, M., Blum, P., et al., 1996. Proc. ODP, Init. Rep. (1182 pp.).

Jordan, R.W., Priddle, J., 1991. Fossil members of the diatom genus *Proboscia*. Diatom Res. 6, 55–61.

Jousé, A.P., 1959. Species novae bacillariophytorum in sedimentis fundi oceani Pacificiet Mario Ochctensis inventae. Novitates Systematicae Plantarum non vascularum. Akad. Sci. SSSR, Inst. Botanicum nomine V. L. Komarovii 3, 12–21.

Keigwin, L.D., 1995. Stable isotope stratigraphy and chronology of the upper Quaternary section at Site 883, Detroit Seamount. Proc. ODP Sci. Results 145, 257–264.

Koç, N., Scherer, R., 1996. Neogene diatom biostratigraphy of the Iceland Sea Site 907. Proc. ODP, Sci. Results 151, 61–74.

Koç, N., Flower, B., 1998. High-resolution Pleistocene diatom biostratigraphy and paleoceanography of Site 919 from the Irminger Basin. Proc. ODP Sci. Results 152, 209–219.

Koç, N., Hodell, D.A., Kleiven, H., Labeyrie, L., 1999. High-resolution Pleistocene diatom biostratigraphy of Site 983 and correlations to isotope stratigraphy. Proc. ODP Sci. Results 162, 51–62.

Koizumi, I., 1986. Pliocene and Pleistocene diatom datum levels related with paleoceanography in the Northwest Pacific. Mar. Micropaleontol. 10, 309–325.

Koizumi, I., Tanimura, I., 1985. Neogene diatom biostratigraphy of the middle latitude western North Pacific, Deep Sea Drilling Project Leg 86. Init. Rep. DSDP 86, 387–407.

Koizumi, I., 1992. Diatom biostratigraphy of the Japan Sea: Leg 127. Proc. ODP Sci. Results 127/128, 249–289.

Larsen, H. C., Saunders, A. D., Clift, P. D. et al., 1994. Proc. ODP, Init. Rep. 152, College Station, TX (Ocean Drilling Program).

Martinson, D.G., Pisias, N.G., Hays, J.D., Imbrie, J., Moore, T.C., Shackleton, N.J., 1987. Age dating and the orbital theory of the ice ages: development of a high-resolution 0 to 300,000 year chronostratigraphy. Quat. Res. 27, 1–29.

McManus, J.F., Oppo, D.W., Cullen, J.L., 1999. A 0.5 million year record of millennial-scale climate variability in the North Atlantic. Science 283, 971–975.

Monjanel, A.-L., Baldauf, J.G., 1989. Miocene to Holocene diatom biostratigraphy from Baffin Bay and Labrador Sea, Ocean Drilling Program Sites 645 and 646. Proc. ODP, Sci. Results 105, 305–322.

Morley, J.J., Hays, J.D., Robertson, J.H., 1982. Stratigraphic framework for the late Pleistocene in the northwest Pacific Ocean. Deep Sea Res. 29, 1485–1499.

Morley, J.J., Tiase, V.L., Ashby, M.M., Kashgarian, M., 1995. High-resolution stratigraphy for Pleistocene sediments from North Pacific Sites 881, 883, and 887 based on abundance variations of the radiolarian *Cycladophora davisiana*. Proc. ODP Sci. Results 145, 133–140.

Myhre, A.M., Thiede, J., Firth, J.V., et al., 1995. Proc. ODP, Init. Rep. (926pp.).

Prell, W., Imbrie, J., Martinson, D.G., Morley, J.J., Pisias, N.G., Shackleton, N.J., Streeter, H.F., 1986. Graphic correlation of oxygen isotope stratigraphy: application to the Late Quaternary. Paleoceanography 1, 137–162.

Sancetta, C., Silvestri, S., 1984. Diatom stratigraphy of the late Pleistocene (Brunhes) subarctic Pacific. Mar. Micropaleontol. 9, 263–274.

Srivastava, S.P., Arthur, M., et al., 1987. Proc. ODP, Init. Rep. 105, College Station, TX (Ocean Drilling Program).

Wold, C.N., 1994. Cenozoic sediment accumulation on drifts in the northern North Atlantic. Paleoceanography 9 (6), 917–941.

Yanagisawa, Y., Akiba, F., 1998. Refined Neogene diatom biostratigraphy for the northwest Pacific around Japan, with an introduction of code numbers for selected diatom biohorizons. J. Geol. Soc. Jpn 104 (6), 395–414.